Biochimica et Biophysica Acta 1817 (2012) 401–409

Contents lists available at SciVerse ScienceDirect

Biochimica et Biophysica Acta

journal homepage: www.elsevier.com/locate/bbabio

Silencing of nicotinamide nucleotide transhydrogenase impairs cellular redox homeostasis and energy metabolism in PC12 cells

Fei Yin, Harsh Sancheti, Enrique Cadenas *

Department of Pharmacology and Pharmaceutical Sciences, School of Pharmacy, University of Southern California, Los Angeles, CA 90089, USA

ARTICLE INFO

Article history:
Received 26 August 2011
Received in revised form 6 December 2011
Accepted 9 December 2011
Available online 16 December 2011

Keywords:
Nicotinamide nucleotide transhydrogenase
Mitochondrion
Bioenergetics
Redox status
JNK
Apoptosis

ABSTRACT

Mitochondrial NADPH generation is largely dependent on the inner-membrane nicotinamide nucleotide transhydrogenase (NNT), which catalyzes the reduction of $NADP^+$ to NADPH utilizing the proton gradient as the driving force and NADH as the electron donor. Small interfering RNA (siRNA) silencing of NNT in PC12 cells results in decreased cellular NADPH levels, altered redox status of the cell in terms of decreased GSH/GSSG ratios and increased H_2O_2 levels, thus leading to an increased redox potential (a more oxidized redox state). NNT knockdown results in a decrease of oxidative phosphorylation while anaerobic glycolysis levels remain unchanged. Decreased oxidative phosphorylation was associated with a) inhibition of mitochondrial pyruvate dehydrogenase (PDH) and succinyl-CoA:3-oxoacid CoA transferase (SCOT) activity; b) reduction of NADH availability, c) decline of mitochondrial membrane potential, and d) decrease of ATP levels. Moreover, the alteration of redox status actually precedes the impairment of mitochondrial bioenergetics. A possible mechanism could be that the activation of the redox-sensitive c-Jun N-terminal kinase (JNK) and its translocation to the mitochondrion leads to the inhibition of PDH (upon phosphorylation) and induction of intrinsic apoptosis, resulting in decreased cell viability. This study supports the notion that oxidized cellular redox state and decline in cellular bioenergetics – as a consequence of NNT knockdown – cannot be viewed as independent events, but rather as an interdependent relationship coordinated by the mitochondrial energy-redox axis. Disruption of electron flux from fuel substrates to redox components due to NNT suppression induces not only mitochondrial dysfunction but also cellular disorders through redox-sensitive signaling.

1. Introduction

Mitochondria integrate distinct cytosolic signaling pathways and generate second messengers (e.g., H_2O_2, NAD^+/NADH, ATP) that are involved in the regulation of redox-sensitive cell signaling. Mitochondrial generation of H_2O_2 is a function of the mitochondrial energy-redox axis: the energy component of this axis is encompassed by the generation of reducing equivalents (NADH) by the tricarboxylic acid cycle and their flow through the respiratory chain with concomitant generation of O_2^- and H_2O_2. The redox component is the domain of H_2O_2 removal systems – mainly glutathione peroxidase and peroxiredoxin 3 – that use GSH and thioredoxin-2 as electron donors; the ultimate reductant for these systems is NADPH (supporting the activities of glutathione reductase and thioredoxin reductase). Hence, the steady-state levels of mitochondrion-generated H_2O_2 in cytosol are largely determined by maintenance of the mitochondrial energy-redox axis.

Mitochondrial NADPH is formed mainly through three pathways (a) $NADP^+$-dependent isocitrate dehydrogenase (IDH2), (b) malic enzyme, and (c) nicotinamide nucleotide transhydrogenase (NNT). Of these pathways, ~50% of the mitochondrial NADPH pool is uncoupler sensitive, thus suggesting that NNT-catalyzed reduction of $NADP^+$ accounts for more than 50% of mitochondrial NADPH pool [1]. NNT – a nuclear encoded mitochondrial 110 kDa protein located on mitochondrial inner membrane [2] – catalyzes the reversible reduction of $NADP^+$ to NADPH and the conversion of NADH to NAD^+ (Eq. (1)). Under physiological conditions,

$$NADH + NADP^+ + H^+_{intermembrane} \leftrightarrow NAD^+ + NADPH + H^+_{matrix} \quad (1)$$

the proton gradient across the mitochondrial inner membrane strongly stimulates the forward reaction, i.e., the generation of NADPH. Under anaerobic and energy-deficient conditions, the reverse reaction catalyzed by NNT, i.e., the generation of NADH, also has transient effects on maintaining mitochondrial membrane potential through NADPH hydrolysis and H^+ pumping, but the contribution of the backward reaction to the proton gradient is probably of little significance under physiological conditions [3].

Abbreviations: NNT, nicotinamide nucleotide transhydrogenase; PDH, pyruvate dehydrogenase; SCOT, succinyl-CoA:3-oxoacid CoA transferase; DCF, 2′,7′-dichlorodihydrofluorescein; OCR, oxygen consumption rate; ECAR, extracellular acidification rate; JNK, c-Jun N-terminal kinases; MnSOD, manganese superoxide dismutase; COX IV, cytochrome c oxidase subunit IV

* Corresponding author at: Pharmacology and Pharmaceutical Sciences, School of Pharmacy, University of Southern California, Los Angeles, CA 90089, USA. Tel.: +1 323 442 1418; fax: +1 323 224 7473.
E-mail address: cadenas@usc.edu (E. Cadenas).

0005-2728/$ – see front matter © 2011 Elsevier B.V. All rights reserved.
doi:10.1016/j.bbabio.2011.12.004

The production of NADPH by NNT requires NADH as electron donor and the proton gradient as driving force. NNT could therefore provide a critical link between the mitochondrial metabolic function and redox homeostasis by coupling NADPH generation to the tricarboxylic acid cycle, active respiration, and O_2^-/H_2O_2 production by electron transfer chain. The crucial role of NNT in the maintenance of the redox environment is revealed by the fact that ablation of NNT renders *C. elegans* more susceptible to oxidative stress and decreases the cellular GSH/GSSG ratio [4]. In mammalians, mice deficient in manganese superoxide dismutase (MnSOD, SOD2) die much earlier if they also lack functional NNT [5]. Moreover, glucose causes a dramatic increase in oxidant levels in β-cells from mice carrying loss-of-function mutants of NNT [6].

Thus, NNT could play a significant role in the maintenance of the mitochondrial energy-redox axis and determine the levels of mitochondrion-generated H_2O_2 in cytosol and its subsequent involvement in domain-specific regulation of redox-sensitive signaling pathways: p38 MAPK, JNK, and other serine kinases are redox-sensitive, although the extent to which H_2O_2 from sources other than mitochondria contribute to their regulation is not clear. The involvement of mitochondrial H_2O_2 in the regulation of JNK, however, has been established as well as the translocation of JNK to the outer mitochondrial membrane in primary cortical neurons and its effects on energy metabolism by triggering pathways that involve inhibition of pyruvate dehydrogenase (PDH) upon phosphorylation of the $E_{1\alpha}$ subunit [7].

This study was aimed at assessing (a) the function of NNT in regulating redox status of the cell; (b) the effect of NNT-regulated redox change on cellular energy metabolism, and (c) at identifying and validating potential mitochondrial-cytosol signaling pathway(s) that are modulated by metabolic or oxidative signals in NNT knockdown cells and that impact the fate of the cell. These aims were performed in PC12 cells transfected with either non-sense siRNA or siRNA against NNT.

2. Materials and methods

2.1. Cell culture

Experiments in this study were performed on rat pheochromocytoma cells (PC12), a dopaminergic cell model with well-defined steps in response to metabolic, oxidative stress-, or apoptotic signals. This cell line enables to investigate the effects of NNT knockdown on cellular redox status, metabolic function and apoptosis, as well as its implications in neurodegeneration. PC12 cells, obtained from American Type Culture Collection, were maintained in RPMI medium 1640 supplemented with 10% horse serum, 5% fetal bovine serum, and 1% penicillin–streptomycin [8]. Cell differentiation was done in differentiation medium (RPMI medium 1640 + 1% donor horse serum + 100 ng/ml nerve growth factor + 50 ng/ml cyclic AMP) for 5 days.

2.2. siRNA transfection

The siRNA sequences against NNT were 5′-ggcggaaacuuugaaacgadTdT-3′ and 5′-ucguuucaaaguuuccgccdGdG-3′ (Ambion). The control siRNA was Silencer Negative Control #3 siRNA (Ambion) composed of a 19 bp scrambled sequence without significant homology to any known genes in rats. After the seeded cells reached 60% confluency, the cells were transfected with non-sense siRNA or siRNA against NNT using oligofectamine transfection reagent (Invitrogen) for 24 h before differentiation.

2.3. Measurement of the redox status of the cell

2.3.1. (a) GSH and GSSG levels

GSH and GSSG concentrations were analyzed using HPLC electrochemical detection [9].

2.3.2. (b) Pyridine nucleotides

NAD^+, NADH, $NADP^+$, and NADPH levels were measured by HPLC [10].

2.3.3. (c) Cellular redox status

The cellular redox status was quantified by the Nernst equation ($E_{hc} = E_0 + 30$ log ([GSSG]/[GSH]^2) where [GSH] and [GSSG] are molar concentrations; E_0 was taken as −264 mV at pH 7.4, as described previously [9,11]. The Nernst potential was calculated from the molar concentration of GSH and GSSG in cell volume at the value of ~10 μl/mg of protein.

2.4. H_2O_2 release and oxygen radical measurement

H_2O_2 generation from PC12 cells was determined by the Amplex Red Hydrogen Peroxide/Peroxidase Assay kit (Invitrogen) following the manufacturer's instructions. For oxygen radical staining, PC12 cells were incubated with 10 μM of cell-permeant H_2DCFDA (2′,7′-dichlorodihydrofluorescein diacetate) for 30 min and 2′,7′-dichlorodihydrofluorescein (DCF) fluorescence was monitored at 495 nm excitation and 520 nm emission.

2.5. Metabolic flux analysis: XF-extraflux analyzer

PC12 cells were cultured on Seahorse XF-24 plates at a density of 5×10^4 cells/well. On the day of metabolic flux analysis, cells were changed to unbuffered DMEM (DMEM base medium supplemented with 25 mM glucose, 2 mM sodium pyruvate, 31 mM NaCl, 2 mM GlutaMax, pH 7.4) and incubated at 37 °C in a non-CO_2 incubator for 1 h. All medium and injection reagents were adjusted to pH 7.4 on the day of assay. Baseline measurements of oxygen consumption rate (OCR, measured by oxygen concentration change) and extracellular acidification rate (ECAR, measured by pH change) were taken before sequential injection of treatments/inhibitors: oligomycin (ATP synthase inhibitor, 4 μM), FCCP (mitochondrial respiration uncoupler, 1 μM), and rotenone (Complex I inhibitor, 1 μM). After the assays, plates were saved and protein readings were measured for each well to confirm equal cell number/well.

2.6. Mitochondrial membrane potential

Mitochondrial membrane potential was determined by measuring the $\Delta\Psi_m$-dependent distribution of JC-1 using a fluorescence spectrometer as described [12].

2.7. Lactic acid and ATP measurements

Differentiated PC 12 cell medium was collected, acidified with an equal volume of perchloric acid (2 M), and centrifuged for 10 min at 12,000 *g*. The supernatant was neutralized with $KHCO_3$ (3 M) and centrifuged at 12,000 *g*. 100 μl of the extract was added to 500 μl of reaction buffer and the concentration of lactic acid was measured in terms of NADH absorbance at 340 nm (assay kit from Abnova). For ATP measurements, cells were lysed using perchloric acid (2 mol/l); cell extracts are neutralized using $KHCO_3$ as described above. ATP in cell extracts was quantitatively measured by a bioluminescence assay that uses recombinant firefly luciferase and D-luciferin (assay kit from Invitrogen).

2.8. Measurement of succinyl-CoA:3-oxoacid CoA transferase (SCOT) activity

SCOT activity was measured as previously described [13]. Briefly, cell lysates were disrupted by sonication and then centrifuged at 10,000 *g* for 20 min. The supernatants were incubated with 50 mM Tris–HCl, 5 mM $MgCl_2$, 4 mM iodoacetamide, 0.2 mM acetoacetate,

and 0.1 mM succinyl-CoA, pH 8.0. Catalytic activity was measured spectrophotometrically at 313 nm.

2.9. Western blotting

Cell lysate was solubilized in SDS sample buffer, separated by Laemmli SDS/PAGE, and transferred onto PVDF membranes. Using appropriate antibodies, the immunoreactive bands were visualized with an enhanced chemiluminescence reagent.

2.10. Apoptosis detection and cell viability assay(

2.10.1. a) Apoptosis detection

Cells were collected and resuspended at a concentration of 10^6 cells/ml in the binding buffer (10 mM HEPES/NaOH (pH 7.4), 140 mM NaCl, 2.5 mM $CaCl_2$) and incubated with FITC conjugated Annexin V and propidium iodide (PI) for 15 min at room temperature. Cell apoptosis was analyzed by FACSDiva (BD Biosciences).

2.10.2. (b) Cell viability

Cell viability was assessed by incubating cells with MTT reagent (5 mg/ml) (Sigma) for 30 min at 37 °C in a humidified 5% CO_2 incubator. The reduced intracellular formazan product was dissolved by replacing 2 ml of differentiation medium with the same volume of DMSO. The absorbance at 590 nm was measured with a microplate reader.

2.11. Statistical analysis

Data are reported as means ± SEM of at least three independent experiments. Significant differences between mean values were determined by Student t-test. Means were considered to be statistically distinct if $P<0.05$.

3. Results

3.1. siRNA knockdown of NNT in PC12 cells

PC12 cells were transfected with siRNA to NNT; a scramble (non-sense) siRNA was used as a negative control. Expression of NNT mRNA was mostly abolished (~80% decrease) by siRNA targeted against it, but was not affected in mock-transfected cells or those transfected with nonsense siRNA (Fig. 1A). Likewise, NNT protein expression was not affected after transfection of non-sense siRNA but was decreased by ~60% after transfection of siRNA against NNT (Fig. 1B). NNT mRNA and proteins were normalized to mitochondrial cytochrome c oxidase subunit IV (COX IV) mRNA and protein levels, respectively.

3.2. NADPH production, H_2O_2 release, and the redox status of the cell

The NADPH/$NADP^+$ ratio in differentiated PC12 cell lysate (collected 6 days after transfection) significantly decreased in siNNT-transfected PC12 cells as compared to that of cells transfected with nonsense siRNA (Fig. 2A), thus suggesting that NNT is an important source of NADPH in mitochondria, and its function can affect the total cellular NADPH and $NADP^+$ pools.

The steady-state level of mitochondrial H_2O_2 ($[H_2O_2]_{ss}$) [14,15], is determined at the equilibrium by its sources (mainly the electron leak in the mitochondrial respiratory chain) and its removal. The latter is driven by mitochondrial thiols (glutathione, thioredoxin) that are supported by the ultimate electron donor, NADPH. H_2O_2 release from PC12 cells with different glucose loadings was assessed by the peroxidase-based Amplex Red method (Fig. 2B): there was no significant difference in H_2O_2 release between NNT knockdown group and control group in low glucose media; at high concentrations of glucose in the media (100 mM), H_2O_2 released from NNT-suppressed cells was about 35% higher than that from control cells, thus indicating a compromised H_2O_2 removal system in NNT-suppressed cells upon increased metabolic loading and H_2O_2 generation. It may be surmised that decreased availability of NADPH after NNT suppression affects the reserved antioxidants capacity of the cell, i.e., H_2O_2 removal. In the control group, high glucose (up to 100 mM) did not induce an increased H_2O_2 release, which suggests that increased H_2O_2 release in NNT-silenced cells is not merely a consequence of high metabolic loading. This is supported by the fact that increased DCF fluorescence was observed in NNT-suppressed cells even at low glucose levels (Fig. 2C). H_2DCFDA is a non-specific oxidant detector, but its good cell penetrability enables the capture of various oxidants intracellularly; hence the difference in cellular oxidant levels in control and NNT-silenced cells can be observed regardless of metabolic loadings. The lack of specificity and accuracy of DCFH in detecting H_2O_2 and other

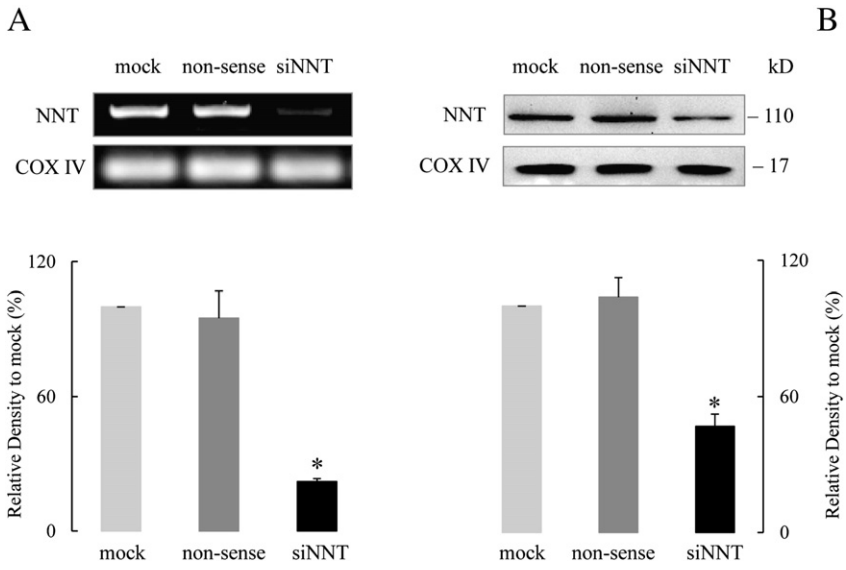

Fig. 1. siRNA knockdown of the NNT gene in PC12 cells. PC 12 cells were transfected with mock, scramble (non-sense) siRNA or NNT siRNA and differentiated for 5 days before RT-PCR and Western blot analyses. A. Upper panel: RT-PCR bands of NNT and COX IV (loading control) mRNA levels; lower panel: relative density of the NNT mRNA level normalized to COX IV. B. Upper panel: Western blots of NNT and COX IV (loading control) protein levels; lower panel: relative density of NNT protein level normalized to COX IV. *$P<0.05$, $n=3$.

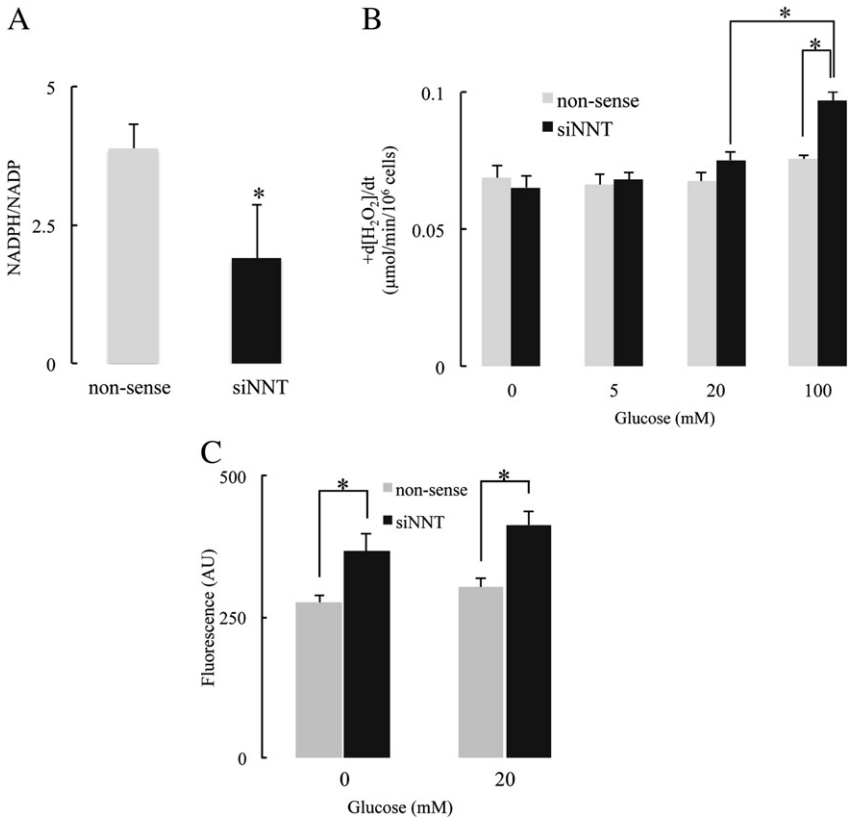

Fig. 2. Effect of NNT knockdown on NADPH production and H_2O_2 release. A. NADPH/$NADP^+$ ratio in differentiated PC12 cells transfected with non-sense or NNT siRNA. The concentration of NADPH and $NADP^+$ in cell lysate was measured by HPLC and the ratio was calculated. B. H_2O_2 release from live PC12 cells with different glucose loadings. H_2O_2 release from PC12 cells incubated in different concentrations of glucose (0–100 mM) was monitored for 30 min using Amplex Red fluorescence dye and the release rate was calculated. C. Non-specific detection of cellular oxidants using H_2DCFDA. PC12 cells stained with H_2DCFDA were incubated with different concentrations of glucose for 30 min and the fluorescence density was measured. *$P<0.05$, $n=4$.

oxidants [16] is recognized here; in these experimental conditions, DCF data confirmed the impairment of cellular antioxidant capacity due to NNT dysfunction in addition to H_2O_2 release data. Because the specific detection of H_2O_2 by Amplex-Red requires horseradish peroxidase (HRP), which is not membrane-permeant, Amplex-Red/HRP can only measure extracellularly diffusing H_2O_2, hence is less sensitive to the fluctuations of intracellular H_2O_2 levels. This could explain the unchanged H_2O_2 release at low glucose concentrations. A high glucose concentration was used to magnify the H_2O_2 production to reveal the impairment of cellular antioxidant defense in NNT-silenced cells, even though this concentration departs from the physiological condition. Taken together, the sole utilization of DCFH or Amplex Red method to detect intracellular oxidant levels has its limitations, either non-specific or insensitive. A combination of both methods can better characterize the cellular level of oxidants tentatively before a specific and in situ detection method is developed.

Increased levels of H_2O_2 can shift the cell from a reduced- to an oxidized state. GSH plays a central and important role in the removal of H_2O_2 generated by the electron transport chain [17,18] and the GSH and GSSG concentrations are determinant of the redox status of the cell. After NNT knockdown, there is a slight decrease of cellular GSH levels and a significant increase of GSSG levels (Table 1). Accordingly, GSH/GSSG ratio decreases from 136.50 ± 32.77 in control cells to 68.78 ± 10.12 in siNNT-transfected cells, thus accounting for a less negative redox potential value in siNNT-transfected cells (-235.40 ± 2.56 mV compared to -245.62 ± 0.67 mV in control cells, Table 1). This indicates the importance of NNT in maintaining the mitochondrial and cellular redox status by regulating NADPH-dependent GSH regeneration.

3.3. Energy metabolism in siNNT-transfected PC12 cells

Mitochondria provide most of the energy needed for cellular functions by the conversion of energy in fuel molecules into ATP through oxidative phosphorylation. Oxygen consumption rate (OCR) by mitochondria reflects the activity of mitochondrial bioenergetics, and is thus an important parameter of mitochondrial function. At 6 days after transfection, siNNT-transfected cells had a substantially lower basal OCR relative to control cells (Fig. 3A); following the addition of oligomycin, OCR declined in both control- (334 pmols/min decrease, ~65% of basal) and siNNT-transfected cells (84 pmols/min decrease, ~50% of basal) (Fig. 3A; 25–50 min), indicating that ATP turnover was significantly lower in NNT knockdown cells than in control cells. Maximal respiratory capacity – measured after the addition of the uncoupler FCCP – was substantially lower in PC12 cells with NNT knocked down (Fig. 3A; 50–75 min). The addition of the Complex I

Table 1
GSH and GSSG levels and the redox potential of the cell.

	Non-sense	siNNT
GSH (nmol/mg protein)	19.20 ± 0.50	16.72 ± 0.84*
GSSG (nmol/mg protein)	0.16 ± 0.03	0.26 ± 0.08*
GSH/GSSG	136.50 ± 32.77	68.78 ± 10.12*
Redox potential (mV)	-245.62 ± 2.56	-235.40 ± 0.67*

PC12 cells were transfected with non-sense or NNT siRNA and differentiated for 5 days before collection. Cell lysates were subjected to HPLC analyses of GSH and GSSG. Concentrations expressed in nmol/cell lysate protein. The redox potential of the cell was estimated by the equation: $E_{hc} = E_0 + 30 \log ([GSSG]/[GSH]^2$.

* $P<0.05$; $n=4$.

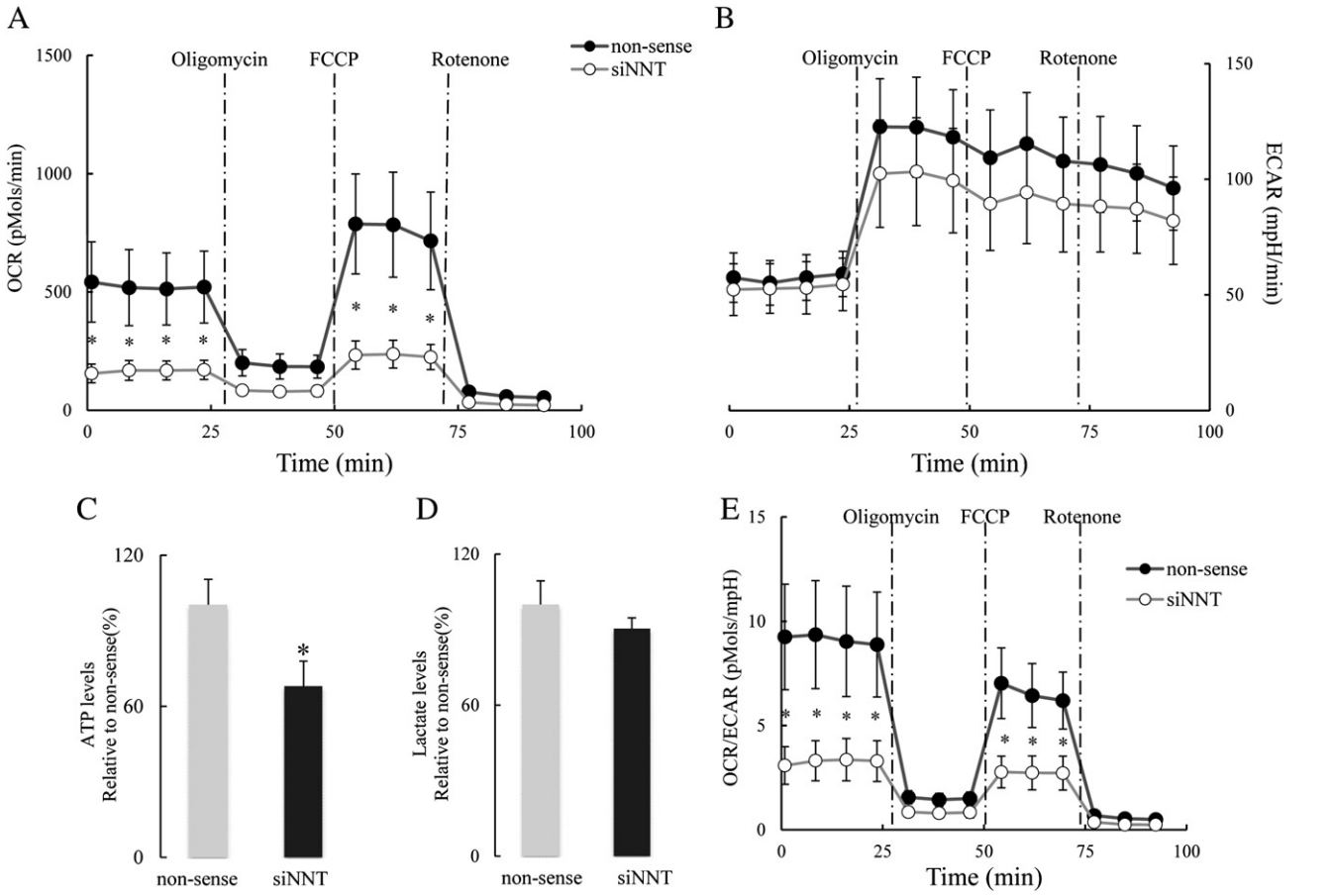

Fig. 3. Cellular energy metabolism in siNNT-transfected PC12 cells. PC12 cells were transfected with non-sense or NNT siRNA and differentiated for 5 days. OCR and ECAR were determined using Seahorse XF-24 Metabolic Flux Analyzer. Vertical dashed lines indicate time of addition of mitochondrial inhibitors: oligomycin (4 μM), FCCP (1 μM), or rotenone (1 μM). A. OCRs in NNT-suppressed cells (open circles) have lower basal rates and maximal rates (after the addition of FCCP) of mitochondrial respiration than those of control cells (filled circles). B. No significant difference in ECAR was observed after NNT knockdown (open circles), compared to control groups (filled circles). C. Cellular ATP levels decreased after NNT knockdown. D. No significant change in extracellular lactate levels was observed in NNT suppressed cells; E. the OCR/ECAR ratio of NNT-suppressed cells (open circles) is lower than that of control group (filled circles) at basal conditions and after the addition of FCCP. $^{*}P<0.05$, $n=5$. OCR, ECAR, ATP and lactate readings were normalized to total protein concentration in each well.

inhibitor rotenone resulted in a further reduction in OCR (12% of basal OCR remained for control and 16% of basal OCR remained for siNNT); the residual O_2 consumption was accounted for by non-mitochondrial O_2-consuming pathways (Fig. 3A; 75–100 min).

Anaerobic glycolysis, the conversion of glucose to lactate, provides a modest amount of ATP. The extracellular acidification rate (ECAR) was used to detect the glycolytic activity by monitoring pH changes due to lactic acid generation. There were no significant differences in ECAR between control and siNNT-transfected cells (Fig. 3B). The increase in ECAR in response to oligomycin (in both siNNT- and non-sense transfected cells) indicated a shift to ATP production by glycolysis via the Pasteur effect [19]. Decreased ATP levels in NNT knockdown cells (Fig. 3C) suggests that the overall energy metabolism is compromised with NNT suppression, because mitochondrial oxidative phosphorylation contributes to the majority of ATP production in the cell; the extracellular lactic acid levels (Fig. 3D) is consistent with the ECAR data indicating an unchanged anaerobic glycolysis rate. Compared to the dramatic decrease in OCR in siNNT-transfected cells, the unchanged ECAR values suggested that a larger proportion of the total cellular ATP was generated through glycolysis. In these experiments, OCR and ECAR values were normalized to total protein concentration in each well. Considering the decrease of cell viability in NNT-suppressed cells (as shown below in Section 3.5), the dramatic decline in mitochondrial respiration should be reflecting the combined effects of impaired mitochondrial function in individual living cells and a decrease of overall cell density. The increased glycolysis level in individual cells was seemingly offset by decreased cell number, which made the final output reading unchanged. Hence, an OCR/ECAR ratio analysis was conducted that confirmed that ratio of O_2 consumption- and extracellular acidification rate were significantly lower in siNNT-transfected PC12 cells (Fig. 3E). Another factor that may be taken into consideration regarding unchanged glycolysis is that some components of the glycolytic machinery in the cytosol are sensitive to redox modification (such as GAPDH [20]) and may thereby be inhibited due to redox state change after NNT knockdown.

3.4. Components in mitochondrial bioenergetics

NNT generates NADPH from $NADP^+$ using NADH as reducing equivalents and proton gradient across mitochondrial inner membrane as the driving force (Fig. 4A). Both, NADH and H^+ gradients are highly involved in mitochondrial energy metabolism. The NADH/NAD^+ values were substantially lower in differentiated siNNT-transfected cells than in control cells (Fig. 4B); suppression of NNT activity resulted in a decline of NADH/NAD^+ ratio (Fig. 4B); likewise, the decrease in $\Delta\Psi_m$ (Fig. 4C) could be a consequence of limited NADH supply. $\Delta\Psi_m$ is established by H^+ pumping along with electron flow through Complexes I–IV of the respiratory chain, and NADH is the initial electron donor.

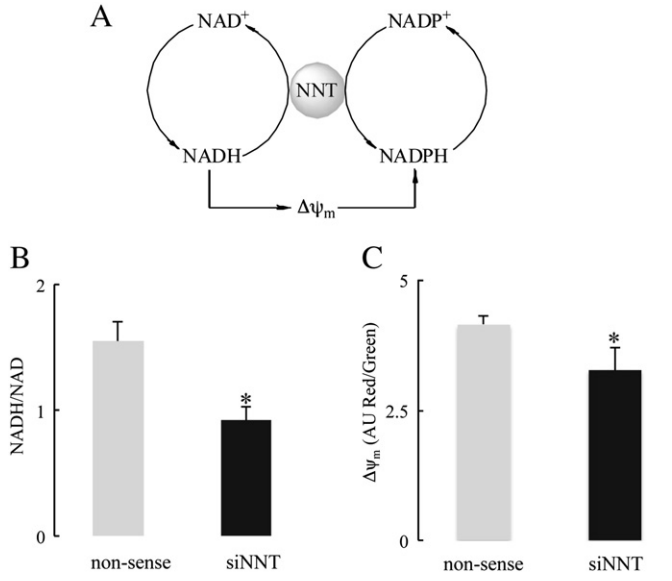

Fig. 4. Effect of NNT knockdown on mitochondrial bioenergetic machinery. A. Schematic representation of the interaction between NNT function and mitochondrial bioenergetic components. NADH generated in TCA cycle can either be used by respiratory chain to build up membrane potential or be used by NNT to reduce $NADP^+$ to NADPH; membrane potential is also the driving force for NNT to generate NADPH in physiological conditions. B. NADH/NAD^+ ratio in differentiated PC12 cells decreases after transfection of NNT siRNA. The concentration of NADH and NAD^+ in cell lysate was measured by HPLC and the ratio was calculated. C. Mitochondrial membrane potential ($\Delta\Psi_m$) is lower in NNT-suppressed cells than control group. PC12 cells were differentiated and stained with JC-1 dye, and the ratio of red and green fluorescence intensity was calculated. *$P<0.05$, $n=4$.

These data suggest that the decreased OCR in siNNT-transfected cells could be ascribed to decreased NADH availability accompanied by a decline in mitochondrial membrane potential. It was expected that suppression of NNT activity would lead to an accumulation of NADH (which is consumed by NNT to generate NADPH in physiological conditions) rather than a decline of NADH. We therefore performed a time-response study analyzing the effect of NNT knockdown on the energy and redox status of the cell. As shown in Fig. 5, 1 day after siNNT transfection, the NADPH/$NADP^+$ ratio has decreased by about 35% (Fig. 5C), while the NADH/NAD^+ ratio increased by about 25% (Fig. 5D). At the same time point, the OCR and ECAR are not changed compared to control group (Fig. 5A, B). These data indicate that the alteration of redox status of the cell precedes the impairment of mitochondrial energy metabolism. The increase in NADH/NAD^+ ratio is in agreement with Eq. (1), i.e., NNT knockdown initially leads to NADPH shortage and NADH accumulation. It may be suggested that indirect effects following NNT suppression are involved in the control of NADH levels in siNNT-transfected cells. In this regard, the pyruvate dehydrogenase (PDH) complex is critical to the cellular energy metabolism inasmuch as it controls the entry of substrates (acetyl-CoA) to the tricarboxylic acid cycle and the further generation of reducing equivalents (NADH). Western blotting showed a substantial increase in the phosphorylated (inactive) form of the $E_{1\alpha}$ subunit of PDH along with a slight decrease in total PDH in siNNT-transfected cells (Fig. 6A), which results in an increased inhibition of PDH (Fig. 6B). The inhibition of PDH activity may account for the decreased NADH/NAD^+ values observed in cells with a diminished NNT activity (Fig. 4B).

Succinyl-CoA-transferase (SCOT) alternatively provides acetyl-CoA to the tricarboxylic acid cycle upon metabolism of ketone bodies (e.g. acetoacetate and β-hydroxybutyrate); SCOT activity was also found to be decreased by ~34% in NNT-transfected cells (Fig. 6C), thus limiting the alternative NADH generation.

Taken together, the decreased NADH/NAD^+ values observed in differentiated cells upon suppression of NNT activity appear to be a consequence of a limited acetyl-CoA supply (and further generation of NADH) to the tricarboxylic acid cycle imposed by an inhibited PDH complex and decreased SCOT activity. This could also account for the substantially diminished OCR and ATP levels in siNNT-transfected cells.

3.5. Activation of JNK and apoptotic pathways

Previous work demonstrated that JNK, a member of the MAPK family, translocates to mitochondria upon activation and initiates a signaling cascade across both mitochondrial membranes resulting in phosphorylation (and inhibition) of mitochondrial matrix PDH [7,21]. Besides, mitochondrion-generated H_2O_2 is involved in the modulation of redox-sensitive cell signaling such as JNK pathway [22–25]; accordingly, the increased H_2O_2 release from NNT-suppressed PC12 cells (Fig. 2B) was associated with JNK1 activation (its phosphorylated form) (Fig. 7A) as well as an increase in p-JNK1/JNK1 values (Fig. 7B). This links the altered mitochondrial redox status to impaired mitochondrial energy metabolism through H_2O_2 levels, JNK activation, and PDH inhibition. The interaction of JNK with mitochondria suggests a network involving cytosolic and mitochondrial processes that control cellular energy levels and the redox environment. Expectedly, these redox-energy changes are associated with a marked decrease in cellular viability (Fig. 7C), partly supported by the effect of JNK on mitochondrion-dependent apoptosis [26–29]. FACS analyses of NNT-suppressed PC12 cells (Fig. 7D) showed a significant higher population of apoptotic cells (early and late stages of apoptosis, Fig. 7E). These results suggest the important role of NNT in the regulation of cellular function though mitochondria-generated H_2O_2 (as second messenger) and redox-sensitive signaling.

4. Discussion

The results reported here with NNT-suppressed PC12 cells showing that NNT plays a critical role in regulating cellular redox status and energy metabolism as well as cytosolic redox-sensitive signal pathways further confirm the significant functional role of NNT as a mitochondrial NADPH source in other organisms or tissues [4,30]. siRNA silencing of NNT in PC12 cells results in decline of NADPH production and an oxidized cellular redox status as inferred by increased GSSG levels, decreased GSH/GSSG ratio, and a less negative redox potential. Furthermore, a decrease in NADPH supply in NNT-knockdown cells results in an augmented H_2O_2 release, consistent with previous reports on an insulin-secreting β-cell line [6], in which an increase in DCF fluorescence was found in $NNT^{-/-}$ β cells at glucose loading of 20 mM.

The consequences of altered redox status on regulation of mitochondrial energy metabolism may be affected through the redox modulation of cytosolic signaling cascades and through redox-mediated post-translational modifications of mitochondrial proteins [31]. The first pathway is primarily through the activation/inhibition of numerous redox-sensitive signaling pathways (such as JNK and other MAPKs) by H_2O_2 released from mitochondria. In the NNT-suppressed PC12 cell model, increased H_2O_2 production from mitochondria and a more oxidized redox environment are associated with activation of cytosolic JNK, which further translocates to mitochondria (as shown with primary cortical neurons [7]) and initiates a phosphorylation cascade that inhibits PDH activity upon phosphorylation of the $E_{1\alpha}$ subunit, thereby increasing energy deficits. SCOT, which catalyzes the rate-limiting step of generation of acetyl-CoA from ketone bodies, also exhibited a lower activity in NNT knockdown cells; previous work in our laboratory showed that SCOT could be post-translationally modified upon altered redox status, either by glutathionylation [32] or nitration [33], and both modifications decreased its activity. Inhibition of PDH and SCOT is expected to lead to a decrease of substrate (i.e., acetyl-CoA) entry into the tricarboxylic acid

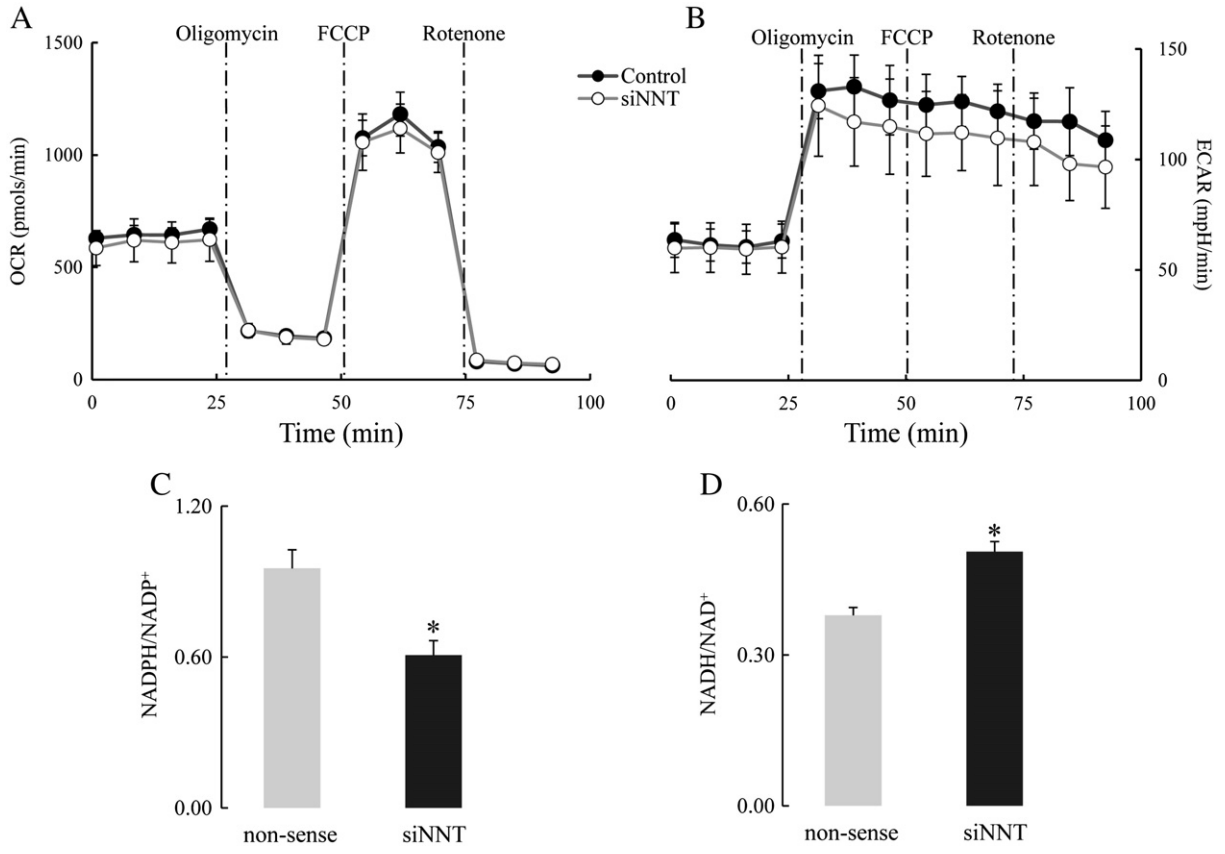

Fig. 5. Alteration of redox status after NNT knockdown precedes the impairment of energy metabolism. 1 day after siNNT transfectioin, OCR and ECAR were determined using Seahorse XF-24 Metabolic Flux Analyzer. Vertical dashed lines indicate time of addition of mitochondrial inhibitors: oligomycin (4 μM), FCCP (1 μM), or rotenone (1 μM). A. OCRs in NNT-suppressed cells (open circles) remain unchanged in basal rates and maximal rates (after the addition of FCCP) of mitochondrial respiration compared to control cells (filled circles). B. No significant difference in ECAR was observed after NNT knockdown (open circles), compared to control groups (filled circles). C. NADPH/NADP$^+$ ratio in differentiated PC12 cells 1 day after transfection with non-sense or NNT siRNA; D. NADH/NAD$^+$ ratio in differentiated PC12 cells 1 day after transfection with non-sense or NNT siRNA.

cycle, thereby limiting the NADH generation, as confirmed by the reduced NADH/NAD$^+$ ratios. A decreased NADH supply to the mitochondrial respiratory chain would also account for the reduced membrane potential and maximal respiratory capacity (Figs. 4C, 3A). The compromised mitochondrial respiration in NNT knockdown PC12 cells (Fig. 3A) is associated with unchanged anaerobic glycolysis levels (Fig. 3B, D), indicating an increased contribution of anaerobic glycolysis to cellular ATP production whereas the total ATP levels are declined (Fig. 3C). A similar shift towards glycolysis was reported in JNK-treated primary cortical neurons with an inhibited PDH activity [7].

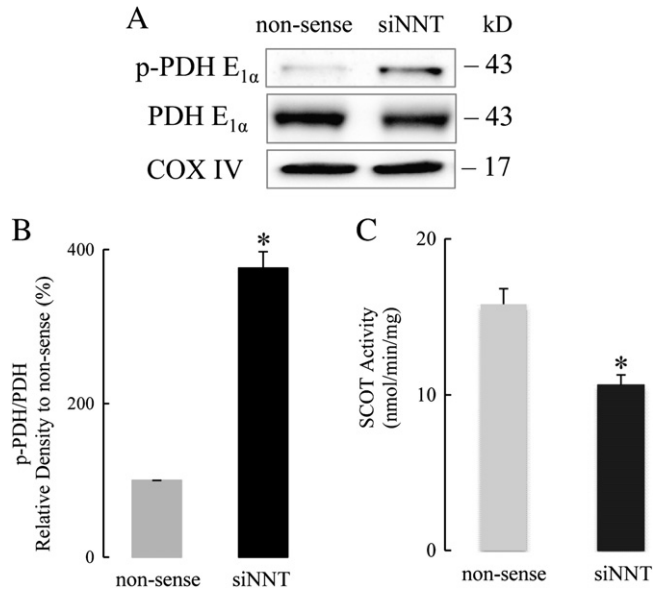

Fig. 6. PDH and SCOT activities in siNNT-transfected PC12 cells. A. Western blots of phospho-PDH-E$_{1\alpha}$ and total PDH-E$_{1\alpha}$ levels. COX IV was used as loading control. B. PDH activity was inhibited after NNT knockdown as shown by significantly increased relative phosphorylation level of PDH-E$_{1\alpha}$. C. SCOT activity was inhibited after NNT siRNA transfection in differentiated PC12 cells. *P<0.05, n = 4.

NNT activity provides a link between the mitochondrial metabolic function (energy-transducing activity) and redox homeostasis by coupling NADPH generation to the tricarboxylic acid cycle and active respiration. Hence, NNT plays a critical role in the maintenance of the mitochondrial energy-redox axis. This supports the notion that decline in cellular bioenergetics and changes in the redox status of the cell cannot be viewed as independent events, but rather as an interdependent relationship centered on the mitochondrial energy-redox axis [31]. Disruption of electron flux from fuel substrates to redox components (as a result of NNT dysfunction) induces not only altered redox status by also impaired energy metabolism. It is also suggested that in addition to mitochondrial energy-transducing capacity and redox homeostasis, impairment of NNT activity also affects the cellular functions through interactive communication between mitochondrion-generated second messengers and cytosolic redox-sensitive signaling. This study shows that the modulation of NNT function could be important in the collective impairments of the interdependent mitochondrial energy-redox axis and the regulation of cytosolic redox-sensitive signaling inherent in several pathophysiological situations. Data obtained in this study potentially explain the underlying mechanisms of the poor response of NNT$^{-/-}$ C57Bl/6J mice to glucose [6], and they also explain the lethal effect of combining a deficiency of both SOD2 and NNT [5].

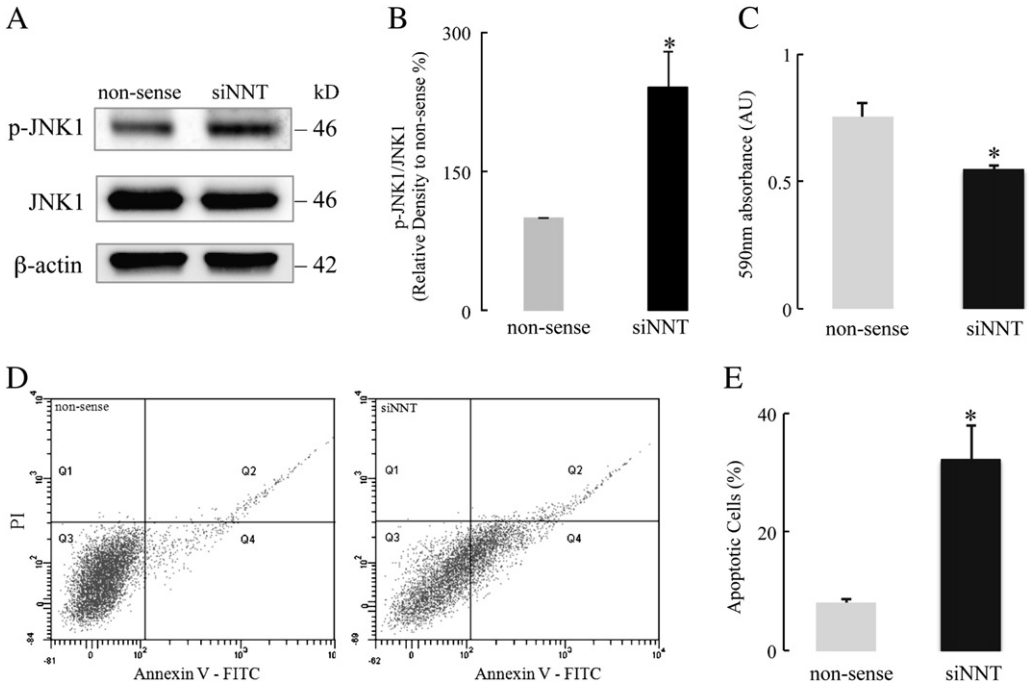

Fig. 7. Activation of JNK and initiation of apoptosis in siNNT-transfected PC12 cells. A. Western blots of phospho-JNK1 and total JNK1 levels. β-actin was used as loading control. B. JNK activity was enhanced after NNT knockdown as shown by its increased relative phosphorylation level. C. Cell viability decreased after NNT siRNA transfection in differentiated PC12 cells using MTT assay at 590 nm. D. Representative image of FACS analyses of apoptosis in PC12 cells using FITC-conjugated AnnexinV and propidium iodide (PI) double staining. E. NNT-suppressed group has more than 4-fold higher population of apoptotic cells as compare with control group. $^{*}P<0.05$, $n=4$.

Moreover, investigations of the physiological and pathological roles of NNT [6] will expand the understanding of the mechanisms that support energy- and/or redox deficits in the early or late stages of some neurodegenerative diseases [21,34,35], diabetes [36,37], cardiovascular disease [30], and aging [38–40].

5. Conclusion

As an important mitochondrial NADPH source, knockdown of NNT alters the mitochondrial and cellular redox status (GSH depletion and H_2O_2 production), along with compromised mitochondrial bioenergetics by inhibition of mitochondrial metabolism (including inhibition of PDH and SCOT activity). The limited NADH availability imposed by inhibition of the latter enzymes could account for the decline of membrane potential, ATP turnover, and maximal respiratory capacity. Activation of redox-sensitive signaling (JNK) by H_2O_2 induces mitochondrion-dependent intrinsic apoptosis and results in decreased cell viability.

Acknowledgements

This work was supported by NIH grant AG016718.

References

[1] J. Rydstrom, Mitochondrial NADPH, transhydrogenase and disease, Biochim. Biophys. Acta 1757 (2006) 721–726.
[2] J.B. Hoek, J. Rydstrom, Physiological roles of nicotinamide nucleotide transhydrogenase, Biochem. J. 254 (1988) 1–10.
[3] W. Ying, NAD+/NADH and NADP+/NADPH in cellular functions and cell death: regulation and biological consequences, Antioxid. Redox Signal. 10 (2008) 179–206.
[4] E.L. Arkblad, S. Tuck, N.B. Pestov, R.I. Dmitriev, M.B. Kostina, J. Stenvall, M. Tranberg, J. Rydstrom, A *Caenorhabditis elegans* mutant lacking functional nicotinamide nucleotide transhydrogenase displays increased sensitivity to oxidative stress, Free Radic. Biol. Med. 38 (2005) 1518–1525.
[5] T.T. Huang, M. Naeemuddin, S. Elchuri, M. Yamaguchi, H.M. Kozy, E.J. Carlson, C.J. Epstein, Genetic modifiers of the phenotype of mice deficient in mitochondrial superoxide dismutase, Hum. Mol. Genet. 15 (2006) 1187–1194.
[6] H. Freeman, K. Shimomura, E. Horner, R.D. Cox, F.M. Ashcroft, Nicotinamide nucleotide transhydrogenase: a key role in insulin secretion, Cell Metab. 3 (2006) 35–45.
[7] Q. Zhou, P.Y. Lam, D. Han, E. Cadenas, c-Jun N-terminal kinase regulates mitochondrial bioenergetics by modulating pyruvate dehydrogenase activity in primary cortical neurons, J. Neurochem. 104 (2008) 325–335.
[8] F. Antunes, D. Han, D. Rettori, E. Cadenas, Mitochondrial damage by nitric oxide is potentiated by dopamine in PC12 cells, Biochim. Biophys. Acta 1556 (2002) 233–238.
[9] L.P. Yap, H. Sancheti, M.D. Ybanez, J. Garcia, E. Cadenas, D. Han, Determination of GSH, GSSG, and GSNO using HPLC with electrochemical detection, Methods Enzymol. 473 (2010) 137–147.
[10] L.K. Klaidman, A.C. Leung, J.D. Adams Jr., High-performance liquid chromatography analysis of oxidized and reduced pyridine dinucleotides in specific brain regions, Anal. Biochem. 228 (1995) 312–317.
[11] D.P. Jones, Redox potential of GSH/GSSG couple: assay and biological significance, Methods Enzymol. 348 (2002) 93–112.
[12] S. Salvioli, A. Ardizzoni, C. Franceschi, A. Cossarizza, JC-1, but not DiOC6(3) or rhodamine 123, is a reliable fluorescent probe to assess delta psi changes in intact cells: implications for studies on mitochondrial functionality during apoptosis, FEBS Lett. 411 (1997) 77–82.
[13] D.H. Williamson, M.W. Bates, M.A. Page, H.A. Krebs, Activities of enzymes involved in acetoacetate utilization in adult mammalian tissues, Biochem. J. 121 (1971) 41–47.
[14] A. Boveris, N. Oshino, B. Chance, The cellular production of hydrogen peroxide, Biochem. J. 128 (1972) 617–630.
[15] A. Boveris, B. Chance, The mitochondrial generation of hydrogen peroxide. General properties and effect of hyperbaric oxygen. Biochem. J. 134 (1973) 707–716.
[16] M.P. Murphy, A. Holmgren, N.G. Larsson, B. Halliwell, C.J. Chang, B. Kalyanaraman, S.G. Rhee, P.J. Thornalley, L. Partridge, D. Gems, T. Nystrom, V. Belousov, P.T. Schumacker, C.C. Winterbourn, Unraveling the biological roles of reactive oxygen species, Cell Metab. 13 (2011) 361–366.
[17] T.R. Hurd, N.J. Costa, C.C. Dahm, S.M. Beer, S.E. Brown, A. Filipovska, M.P. Murphy, Glutathionylation of mitochondrial proteins, Antioxid. Redox Signal. 7 (2005) 999–1010.
[18] B. Chance, H. Sies, A. Boveris, Hydroperoxide metabolism in mammalian organs, Physiol. Rev. 59 (1979) 527–605.
[19] M. Guppy, L. Abas, P.G. Arthur, M.E. Whisson, The Pasteur effect in human platelets: implications for storage and metabolic control, Br. J. Haematol. 91 (1995) 752–757.
[20] L.P. Yap, J.V. Garcia, D.S. Han, E. Cadenas, Role of nitric oxide-mediated glutathionylation in neuronal function: potential regulation of energy utilization, Biochem. J. 428 (2010) 85–93.
[21] Q. Zhou, P.Y. Lam, D. Han, E. Cadenas, Activation of c-Jun-N-terminal kinase and decline of mitochondrial pyruvate dehydrogenase activity during brain aging, FEBS Lett. 583 (2009) 1132–1140.
[22] M. Saitoh, H. Nishitoh, M. Fujii, K. Takeda, K. Tobiume, Y. Sawada, M. Kawabata, K. Miyazono, H. Ichijo, Mammalian thioredoxin is a direct inhibitor of apoptosis signal-regulating kinase (ASK) 1, EMBO J. 17 (1998) 2596–2606.
[23] Y.R. Chen, A. Shrivastava, T.H. Tan, Down-regulation of the c-Jun N-terminal kinase (JNK) phosphatase M3/6 and activation of JNK by hydrogen peroxide and pyrrolidine dithiocarbamate, Oncogene 20 (2001) 367–374.

[24] T.D. Foley, J.J. Armstrong, B.R. Kupchak, Identification and H_2O_2 sensitivity of the major constitutive MAPK phosphatase from rat brain, Biochem. Biophys. Res. Commun. 315 (2004) 568–574.
[25] S. Nemoto, K. Takeda, Z.X. Yu, V.J. Ferrans, T. Finkel, Role for mitochondrial oxidants as regulators of cellular metabolism, Mol. Cell. Biol. 20 (2000) 7311–7318.
[26] C.A. Harris, M. Deshmukh, B. Tsui-Pierchala, A.C. Maroney, E.M.J. Johnson, Inhibition of the c-Jun N-terminal kinase signaling pathway by the mixed lineage kinase inhibitor CEP-1347 (KT7515) preserves metabolism and growth of trophic factor-deprived neurons, J. Neurosci. 22 (2002) 103–113.
[27] G.V. Putcha, M. Deshmukh, E.M.J. Johnson, BAX translocation is a critical event in neuronal apoptosis: regulation by neuroprotectants, BCL-2, and caspases, J. Neurosci. 19 (1999) 7476–7485.
[28] S. Kharbanda, S. Saxena, K. Yoshida, P. Pandey, M. Kaneki, Q.Z. Wang, K. Cheng, Y.N. Chen, A. Campbell, T. Sudha, Z.M. Yuan, J. Narula, R. Weichselbaum, C. Nalin, D. Kufe, Translocation of SAPK/JNK to mitochondria and interaction with Bcl-x(L) in response to DNA damage, J. Biol. Chem. 275 (2000) 322–327.
[29] H. Schroeter, C.S. Boyd, R. Ahmed, J.P. Spencer, R.F. Duncan, C. Rice-Evans, E. Cadenas, c-Jun N-terminal kinase (JNK)-mediated modulation of brain mitochondria function: new target proteins for JNK signalling in mitochondrion-dependent apoptosis, Biochem. J. 372 (2003) 359–369.
[30] F.L. Sheeran, J. Rydstrom, M.I. Shakhparonov, N.B. Pestov, S. Pepe, Diminished NADPH transhydrogenase activity and mitochondrial redox regulation in human failing myocardium, Biochim. Biophys. Acta 1797 (2010) 1138–1148.
[31] L.P. Yap, J.V. Garcia, D. Han, E. Cadenas, The energy-redox axis in aging and age-related neurodegeneration, Adv. Drug Deliv. Rev. 61 (2009) 1283–1298.
[32] J. Garcia, D. Han, H. Sancheti, L.P. Yap, N. Kaplowitz, E. Cadenas, Regulation of mitochondrial glutathione redox status and protein glutathionylation by respiratory substrates, J. Biol. Chem. 285 (2010) 39646–39654.
[33] P.Y. Lam, F. Yin, R.T. Hamilton, A. Boveris, E. Cadenas, Elevated neuronal nitric oxide synthase expression during ageing and mitochondrial energy production, Free. Radic. Res. 43 (2009) 431–439.
[34] J. Yao, R.W. Irwin, L. Zhao, J. Nilsen, R.T. Hamilton, R.D. Brinton, Mitochondrial bioenergetic deficit precedes Alzheimer's pathology in female mouse model of Alzheimer's disease, Proc. Natl. Acad. Sci. U. S. A. 106 (2009) 14670–14675.
[35] M.T. Lin, M.F. Beal, Mitochondrial dysfunction and oxidative stress in neurodegenerative diseases, Nature 443 (2006) 787–795.
[36] H. Kaneto, D. Kawamori, T.A. Matsuoka, Y. Kajimoto, Y. Yamasaki, Oxidative stress and pancreatic beta-cell dysfunction, Am. J. Ther. 12 (2005) 529–533.
[37] B.B. Lowell, G.I. Shulman, Mitochondrial dysfunction and type 2 diabetes, Science 307 (2005) 384–387.
[38] M.P. Mattson, T. Magnus, Ageing and neuronal vulnerability, Nat. Rev. Neurosci. 7 (2006) 278–294.
[39] H. Van Remmen, D.P. Jones, Current thoughts on the role of mitochondria and free radicals in the biology of aging, J. Gerontol. A Biol. Sci. Med. Sci. 64 (2009) 171–174.
[40] A. Navarro, A. Boveris, The mitochondrial energy transduction system and the aging process, Am. J. Physiol. Cell Physiol. 292 (2007) C670–C686.